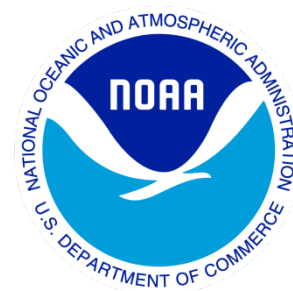


---

# Climate Data Record (CDR) Program

## Climate Algorithm Theoretical Basis Document (C-ATBD)

### Mean Layer Temperature – UCAR (Upper Trop & Lower Strat)



CDR Program Document Number: CDRP-ATBD-0415  
Configuration Item Number: 01B-14  
Revision 2 / June 10, 2015

### REVISION HISTORY

<b>Rev.</b>	<b>Author</b>	<b>DSR No.</b>	<b>Description</b>	<b>Date</b>
1	Shu-peng Ben Ho	DSR-488	Initial Submission to CDR Program	08/26/2013
2	Shu-peng Ben Ho	DSR-882	Extension of POR historically	06/10/2015

## TABLE of CONTENTS

<b>1. INTRODUCTION.....</b>	<b>6</b>
1.1 Purpose .....	6
1.2 Definitions.....	6
1.3 Referencing this Document .....	6
1.4 Document Maintenance.....	7
<b>2. OBSERVING SYSTEMS OVERVIEW.....</b>	<b>8</b>
2.1 Products Generated .....	8
2.2 Instrument Characteristics .....	8
<b>3. ALGORITHM DESCRIPTION.....</b>	<b>10</b>
3.1 Algorithm Overview .....	10
3.2 Processing Outline.....	10
3.3 Algorithm Input.....	14
3.3.1 Primary Sensor Data .....	14
3.3.2 Ancillary Data.....	14
3.3.3 Derived Data .....	14
3.3.4 Forward Models.....	16
3.4 Theoretical Description .....	17
3.4.1 Physical and Mathematical Description.....	17
3.4.2 Data Merging Strategy.....	21
3.4.3 Numerical Strategy .....	21
3.4.4 Calculations.....	21
3.4.5 Look-Up Table Description.....	21
3.4.6 Parameterization .....	21
3.4.7 Algorithm Output.....	21
<b>4. TEST DATASETS AND OUTPUTS.....</b>	<b>22</b>
4.1 Test Input Datasets .....	22
4.2 Test Output Analysis .....	22
4.2.1 Reproducibility.....	22
4.2.2 Precision and Accuracy .....	22
4.2.3 Error Budget.....	24
<b>5. PRACTICAL CONSIDERATIONS.....</b>	<b>25</b>
5.1 Numerical Computation Considerations.....	25
5.2 Programming and Procedural Considerations .....	25
5.3 Quality Assessment and Diagnostics .....	25
5.4 Exception Handling .....	27
5.5 Algorithm Validation .....	27
5.6 Processing Environment and Resources .....	28
<b>6. ASSUMPTIONS AND LIMITATIONS .....</b>	<b>29</b>
6.1 Algorithm Performance.....	29

**6.2    Sensor Performance..... 29**

**7.    FUTURE ENHANCEMENTS..... 30**

**7.1    Enhancement 1- Improve Algorithm Usage ..... 30**

**7.2    Enhancement 2– Further Validation..... 30**

**8.    REFERENCES..... 31**

**APPENDIX A.    ACRONYMS AND ABBREVIATIONS..... 33**

## LIST of FIGURES

Figure 1: Flow chart of processing steps to using radiosonde simulated AMSU TLS (channel 7) to calibrate AMSU data from multiple AMSU missions and construct the Mean Layer Temperature – UCAR (Upper Trop & Lower Strat) Climate Data Record.....	13
Figure 2: AMSU Channel 7 Atmospheric weighting functions for a typical atmospheric profile in the Tropics and the Arctic, respectively. The weighting function is defined as $d(\text{transmittance})/d\ln(p)$ . .....	15
Figure 3: Flow chart of the procedures to use radiosonde data to AMSU forward model to compute the simulated AMSU Channel 7 Tbs. ....	17
Figure 4: Temperature comparisons between COSMIC and radiosonde at 150 hPa for Vaisala-RS92 from 2002 to 2008. The red dot is for the mean difference, the orange line is for the standard deviation, and the dotted line is the sample number for RO and radiosonde pairs in that height. ....	19
Figure 5: Comparison of synthetic RAOB Tbs and (a) AMSU N15 Ch7 Tbs, (b) AMSU N16 Ch7 Tbs, (c) AMSU N18 Ch7 Tbs. ....	24
Figure 6: The differences of temperature between RS92 and collocated GPS RO at 50 hPa for the global (upper left panel), 90°N to 60°N zone (upper right panel), 20°N to 60°N zone (middle left panel), 20°N to 20°S zone (middle right panel), 60°S to 20°S zone (lower left panel), and 90°S to 60°S zone (lower right panel). The red dots are for the day time RS92-RO temperature biases and the blues dots are for the night time RS92-RO temperature biases. ....	26
Figure 7: The time series of MSU/AMSU TTS Tbs between N6-TIROS, N7-N6, N8-N7, N9-N8, N10-N9, N11-N10, N12-N11, N14-N12, N16-N15, N18-N15, N19-N15, Metop-A – N15 for the global (upper left panel), 90° N to 60° N zone (upper right panel), 2° N to 60° N zone (middle left panel), 20° N to 20° S zone (middle right panel), 60°S to 20° S zone (lower left panel), and 90° S to 60° S zone (lower right panel). ....	28

# 1. Introduction

## 1.1 Purpose

The purpose of this document is to describe the algorithm submitted to the National Centers for Environmental Information (NCEI) by Dr. Shu-peng Ben Ho/COSMIC UCAR. This algorithm produces Advanced Microwave Sounder Unit (AMSU) and Microwave Sounder Unit (MSU) Temperatures of Troposphere / Stratosphere (TTS) (AMSU channel 7 and MSU channel 3) from National Oceanic and Atmospheric Administration (NOAA) and Europe METeorological Operational satellite-A (Metop/A) satellites. High quality radiosonde observations (RAOBs) identified by coincident Global Positioning System (GPS) Radio Occultation (RO) temperature profile measurements from Constellation Observing System for Meteorology, Ionosphere, and Climate (COSMIC) and Challenging Mini-satellite Payload (CHAMP) are used to calibrate the AMSU channel 7 measurements from multiple NOAA and Metop-A missions. The calibrated AMSU TTS from 2001 to 2014 are then used to calibrate MSU TTS in the same time period and then the calibrated MSU TTS are used to calibrate those overlapped MSU TTS from 1980 to 2001. The actual algorithm is defined by the computer program (CDR\_ch7\_V2.0 package) that accompanies this document, and thus the intent here is to provide a guide to understanding that algorithm, from both a scientific perspective and in order to assist a software engineer or end-user performing an evaluation of the code.

## 1.2 Definitions

Following is a summary of the symbols used to define the algorithm.

Atmospheric parameters:

$T = \text{Temperature}$  (1)

$P = \text{Pressure}$  (2)

$P_w = \text{Vapor Pressure}$  (3)

$N = \text{Refractivity}$  (4)

$T_b = \text{Brightness Temperature}$  (5)

## 1.3 Referencing this Document

This document should be referenced as follows:

Mean Layer Temperature – UCAR (Upper Trop & Lower Strat) - Climate Algorithm Theoretical Basis Document, NOAA Climate Data Record Program CDRP-ATBD-0415 Rev. 2 (2015). Available at <http://www.ncdc.noaa.gov/cdr/operationalcdrs.html>

## **1.4 Document Maintenance**

This document describes the submission, version 2.0, of the processing algorithm and resulting data. The version number will be incremented for any subsequent enhancements or revisions.

## **2. Observing Systems Overview**

### **2.1 Products Generated**

The objective of this algorithm is to use GPS RO data to identify high quality RAOBs and use the RO identified RAOBs to calibrate AMSU TTS measurements from 2001 to 2014. The calibrated AMSU TTS from 2001 to 2014 are then used to calibrate MSU TTS in the same time period and then the calibrated MSU TTS are used to calibrate those overlapped MSU TTS from 1980 to 2001. Monthly averages over a 34-year period from 1980 through December 2014 from the combined contributions of MSU and AMSU measurements from NOAA and MetOp-A polar orbiters are calculated on a 2.5 degree x 2.5 degree grid. The final product consists of monthly mean averages of calibrated AMSU/MSU TTS measurements, a mean monthly climatology calculated using 33 full years of data, and monthly anomaly values.

### **2.2 Instrument Characteristics**

Accurate RO retrievals of atmospheric variable profiles depend on the adequate calculation of the GPS excess atmospheric phase data of two L band frequencies (1575.42 MHz (L1) and 1227.6 MHz (L2)) due to signal delay and bending in the Earth's atmosphere and ionosphere (Kursinski et al., 1997; Ho et al., 2009a). GPS RO is the only self-calibrated observing technique from space where its fundamental measurement is traceable to the international system of units (SI traceability; Ohring et al., 2007). Because the quality of COSMIC RO data are not affected by the surrounding environment (e.g., geo-location, day and night, etc.), GPS RO data are very useful to identify the possible radiative biases of radiosondes from the 8 km to 25 km altitudes, where radiosonde sensor characteristics vary considerably in times and locations for different sensor types. We have identified radiosonde types whose temperature biases are small in the region from 8 km to 25 km altitude. Then we use the temperature profiles (i.e., from 25 km to surface, see AMSU channel 7 weighting function in Figure 2) from those RO identified radiosonde to simulate the AMSU TTS. Because the RAOB radiative biases are in general higher in the higher altitudes, the radiosonde types with small RO-RAOB biases in the lower stratosphere shall give good temperature in the troposphere.

Globally, there are roughly 850 radiosonde stations using about fourteen different types of radiosonde systems. Different radiosonde systems have their own known observational errors. Because radiosonde sensor characteristics can be affected by the changing environment, the accuracy of radiosonde temperature and water vapor measurement also varies considerably in times and locations for different sensor types (He et al., 2009).



On board the NOAA series of polar-orbiting satellites, the Microwave Sounding Unit (MSU) and the Advanced Microwave Sounding Unit (AMSU) have also provided near all-weather temperature measurements at different atmospheric vertical layers since 1979 and 1998, respectively. With center frequencies located at the oxygen bands ranging between 50 GHz and 58 GHz, the MSU and AMSU instruments are able to provide near all-weather temperature measurements for the lower troposphere (MSU Ch2/AMSU Ch5), the troposphere and stratosphere (MSU Ch3/AMSU Ch7), and the upper troposphere and lower stratosphere (MSU Ch4/AMSU Ch9). Because MSU/AMSU instruments are not originally designed for long-term climate monitoring, the onboard calibration target temperature may drift from orbit to orbit. The radiance biases caused by instrument calibration errors are usually unavoidable and vary for different MSU/AMSU sensors.

## 3. Algorithm Description

### 3.1 Algorithm Overview

The processing of calibrated MSU/AMSU data is achieved by the sequential application of programs, which are divided into three logical steps. First, pixel data of radiances for MSU channel 3 and AMSU channel 7 are extracted from the level 1B data sets and stored in daily files for each polar orbiter. In the second step, the MSU channel 3 brightness temperatures for TIROS, NOAA6 (N6), NOAA7 (N7), NOAA8 (N8), NOAA9 (N9), NOAA10 (N10), NOAA11 (N11), NOAA12 (N12), and NOAA14 (N14) are rebuilt and calibrated by simulated brightness temperatures from radiosonde identified by GPS RO data. Calibration coefficients are calculated from coincident measurements of AMSU channel 7 brightness temperatures and corresponding values derived from an AMSU forward model applied to temperature profile measurements from RO identified radiosondes. In the third step, the monthly calibration coefficients are applied to adjust the AMSU TTS measurements for each polar orbiter to the temperature profiles from the RO identified RAOBs. The calibrated AMSU measurements are then combined into a single dataset of gridded monthly values. From these the climatology is calculated using 33 years of data. AMSU data from N15, N6, N18, N19, and Metop-A and MSU data from TIROS, N6, N7, N8, N9, N10, N11, N12, and N14 are used in this study. The monthly gridded brightness temperatures are generated. For the final step, the climatology is calculated using 33 years of data. Anomaly values are then obtained by subtracting this climatology from the monthly values. The values are saved in netCDF files.

### 3.2 Processing Outline

The three processing steps are indicated in Figure 1. Input data are indicated in the blue boxes. The steps leading to the final output product indicated by the green box are:

**STEP(1) Pre-Processing:** The level 1B data from the polar orbiters are extracted using two IDL (Interface description language) programs. Data from MSU orbiters are obtained from the program 'extract\_msu\_coef.pro'. Data from AMSU orbiters are obtained from the program 'extract\_msu\_bt.pro'.

**STEP(2) Calibration of MSU/AMSU brightness temperatures:** For radiosonde data, channel 7 brightness temperatures ( $T_b$ ) are calculated from vertical profiles of temperature using an AMSU forward model (see Figure 2). The Modern-ERA Retrospective analysis for Research and Applications (MERRA) reanalysis data in HDF format are firstly read and converted to ASCII file by 'merra\_hdf2sav.pro' and 'merra\_sav2txt.pro'. Then the profiles are used to simulate the AMSU channel 7 and MSU channel 3 brightness temperatures for later use.

The set of MSU measurements between overlapping NOAA polar orbiters are co-located with these derived values obtained from the IDL program '*match noaa msu.pro*'. The user must edit this program to specify the names of NOAA orbiter, the time interval of data to process, and the tolerances used to determine coincidence. The program is then compiled and run separately in IDL for each combination of overlapping NOAA orbiters to obtain daily matched measurements. The criteria used to obtain coincident values are 15 minutes in time, 200 km spatial distance, and a scan angle tolerance of 15 degrees. The resulting matched data are stored in daily netCDF files for later use.

Once these datasets are generated for every overlapping polar orbiters, the NOAA14 is selected as the reference missions to calibrate other MSU missions. The offsets are assumed as zero for the reference missions. Eleven nonlinear coefficients are assumed for the reference missions. Then simultaneous nadir overpass (SNO) matching data sets are generated from the matched data files by IDL program '*sno\_step1\_preparematchup\_msu.pro*'. The user must edit the program to specify the matched orbiter names to process. The SNO matchups are used to generate offsets and nonlinear coefficients for other missions by IDL program '*sno\_step2\_soluteequation\_msu.pro*'. The offsets and nonlinear coefficients are then used to rebuild the brightness temperatures for all the missions by IDL program '*sno\_step3\_rebuild\_msu.pro*'.

Then the MERRA simulated hourly gridded Tbs are used for limb correction and location time correction of MSU brightness temperatures. The MERRA MSU channel 3 Tbs are converted to AMSU channel 7 Tbs. The Tbs are also binned and saved in netCDF files for later use. These calibration using MERRA are done by '*sno\_step3\_cnadir\_dbin\_msu.pro*'.

The daily zonal mean inter-satellite biases are generated by '*sno\_step4\_intersatbias\_msu.pro*'. The biases between NOAA14 and radiosonde are also generated by '*sno\_step4\_satraobbias.pro*'. Then the modified Christy methods (Christy et al. 2000, 2003) are used to generate the calibration coefficients to remove the inter-satellite biases, seasonal variations, and trends of biases for all the orbiters by IDL programs '*sno\_step5\_christycorr\_msu.pro*'. Then the coefficients are used to generate 11 groups of Tbs for all the assumed nonlinear coefficients for reference missions by '*sno\_step6\_christyprod\_msu.pro*'. Then the new inter-satellite biases are generated by '*sno\_step7\_new\_intersatbias\_msu.pro*'. The best results are selected from the 11 groups of the Tbs with the smallest standard deviations of inter-satellite biases by IDL programs '*sno\_step8\_select\_msu.pro*'. Then the best results are read and saved in netCDF files by IDL programs '*msu\_daily\_product.pro*'. The daily calibrated results are combined and converted to monthly products by '*msu\_monthly\_product.pro*'.

For AMSU the measurements from each NOAA polar orbiter that are coincident with these derived values are obtained from the IDL program '*match raob noaa.pro*'. The program is then compiled and run separately in IDL for each combination of NOAA

orbiter to obtain daily matched measurements. The criteria used to obtain coincident values are 30 minutes in time, 50 km spatial distance, and a scan angle tolerance of 15 degrees. The resulting matched data are stored in daily ASCII files for later use.

Once these datasets for each polar orbiter have been generated, the coincident measurements from radiosondes are used to calculate the monthly calibration coefficients for each individual polar orbiter.

For the NOAA and METOP-A orbiter, the matched measurements are used to calculate linear fit coefficients for each month using the IDL program '*offset\_slope\_raob\_noaa\_month.pro*'. The program is then compiled and run separately in IDL for each orbiter to store the monthly fit coefficients. The resulting monthly fit coefficients for each orbiter are stored in ASCII files for later use. Five types of radiosonde (RS80 57H, RS80 Loran/DigiCore I II or Marwin, RS92 DigiCore I II OR Marwin, RS92 DigiCore III, RS92 Autosonde) which have been verified by GPS-RO are used in calculating the calibration coefficients.

Because the radionsonde stations are mostly located in tropical and north hemisphere, the linear fit coefficients have to be processed by the IDL program '*offset\_slope\_raob\_noaa\_month\_modify.pro*'.

Prior to applying the linear calibration, monthly means of AMSU channel 7 brightness temperatures for each NOAA orbiter on a 2.5 degree x 2.5 degree grid are calculated by the IDL program '*bin\_noaa\_monthlymean.pro*'. The program is then compiled and run to generate the monthly mean data files for each orbiter.

The calibration coefficients for each polar orbiter are then applied to the monthly mean gridded values to obtain the monthly adjusted AMSU channel 7 brightness temperatures. The program, '*convert\_amsu\_byraob.pro*', which is compiled and run separately for each orbiter, reads in the linear fit coefficients and uses them to adjust the corresponding monthly gridded values. The adjusted monthly mean grids are then stored in ASCII files for later use.

Once all of the monthly gridded values have been calibrated, the IDL program '*combine\_amsu.pro*' reads in the monthly gridded values for the specified set of polar orbiters and averages the values to generate combined monthly gridded values for AMSU channel 7.

**STEP(3) Apply Calibration:** Once all of the monthly gridded values have been generated, the IDL program '*gen\_product.pro*' reads in the monthly gridded Tbs, and generates the climatology and anomaly values. The results are written to the final V4 netCDF datasets.

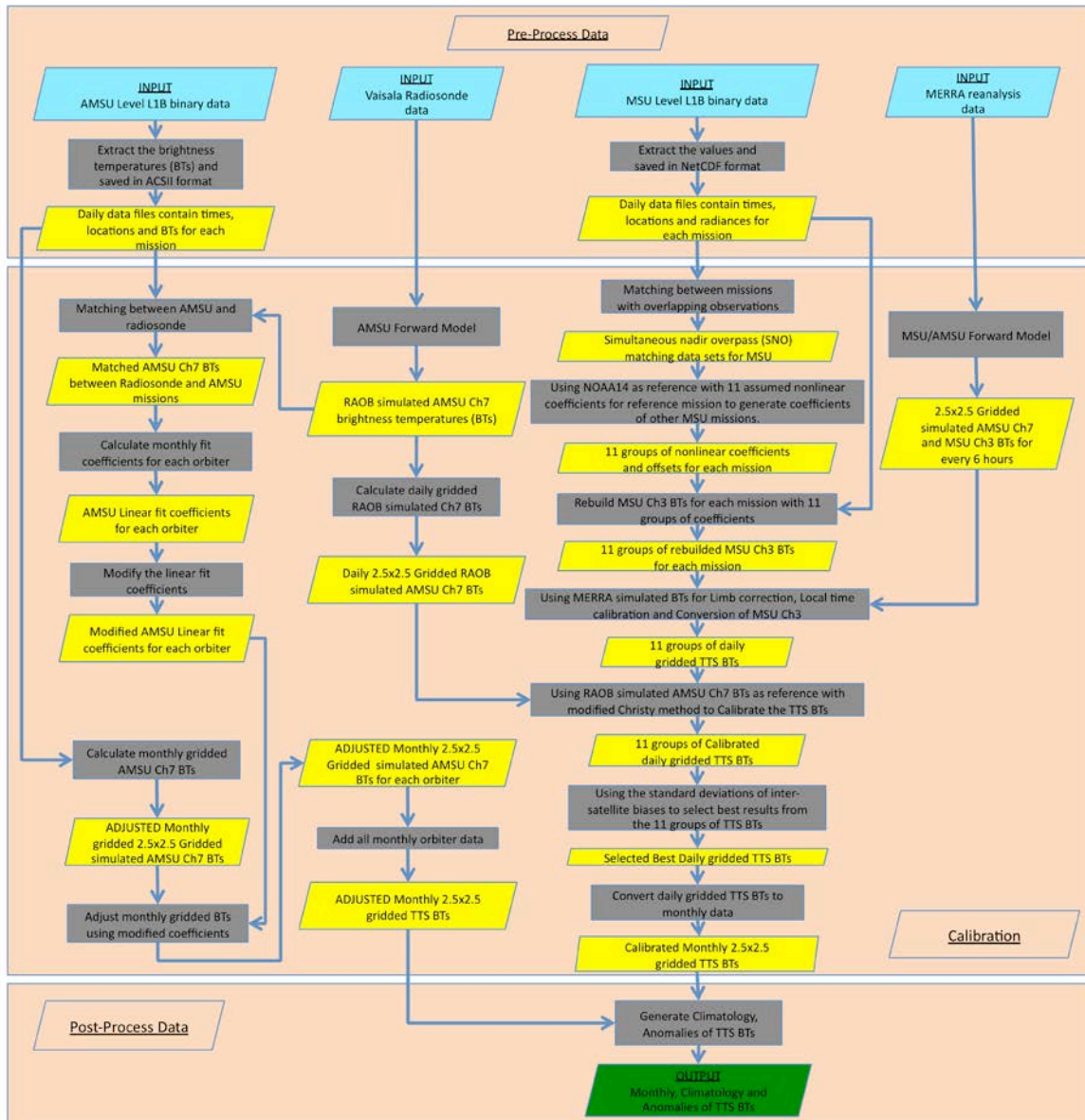


**Figure 1: Flow chart of processing steps to using radiosonde simulated AMSU TLS (channel 7) to calibrate AMSU data from multiple AMSU missions and construct the Mean Layer Temperature – UCAR (Upper Trop & Lower Strat) Climate Data Record.**

## 3.3 Algorithm Input

### 3.3.1 Primary Sensor Data

Level 1B AMSU data from NOAA 15, 16, 18, and 19, and from METOP/A and MSU data from TIROS, N6, N7, N8, N9, N10, N11, N12, and N14 are used. For each orbiter, AMSU channel 7 and MSU channel 3 brightness temperature, latitude, longitude, time, and scan angle values are input into the algorithm. AMSU level 1B data for NOAA and METOP orbiters are available from the NOAA website <http://www.class.noaa.gov/nsaa/products/welcome>.

The radiosonde profiles are extracted from NCEP ADP Global Upper Air Observational Weather Data (ds351.0). The data format is WMO BUFR (<http://rda.ucar.edu/#BUFR>). The NCEP BUFRLIB software (<http://www.nco.ncep.noaa.gov/sib/decoders/BUFRLIB/>) are use to decode BUFR messages and extract the radiosonde profiles. Then the radiosonde profiles are interpolated to 100 pressure levels and then passed to an AMSU forward model to calculate the corresponding channel 7 brightness temperatures. Those derived brightness temperatures, along with latitude, longitude, and time values, are then input into the algorithm. The size of the derived datasets varies with the number of measurements, typically they require about 10 mb per month. All the BUFR data were downloaded from the CISL Research Data Archive <http://rda.ucar.edu/datasets/ds351.0/>.

The MERRA reanalysis data are read and interpolated to 100 pressure levels. Then the profiles are passed to AMSU and MSU forward model to calculate the corresponding AMSU channel 7 and MSU channel 3 brightness temperatures. The MERRA data are available in the NASA website

(<ftp://goldsmr3.sci.gsfc.nasa.gov:/data/s4pa/MERRA/MAI3CPASM.5.2.0/>)

### 3.3.2 Ancillary Data

*N/A*

### 3.3.3 Derived Data

The shape and the magnitude of MSU/AMSU temperature weighting function (WF) is a function of the temperature profile (Fig. 2), so using a MSU or AMSU forward model enables one to reduce WF representation errors in the simulated Tbs as compared to those computed from a globally-fixed WF. The forward model MWF<sub>CIMSS</sub> from the Cooperative Institute for Meteorological Satellite Studies (CIMSS) was operationally employed in the International ATOVS Processing Package developed at Space Science Engineer Center

(SSEC), University of Wisconsin. The validation of microwave transmittance of this model is described in Woolf et al. 1999.

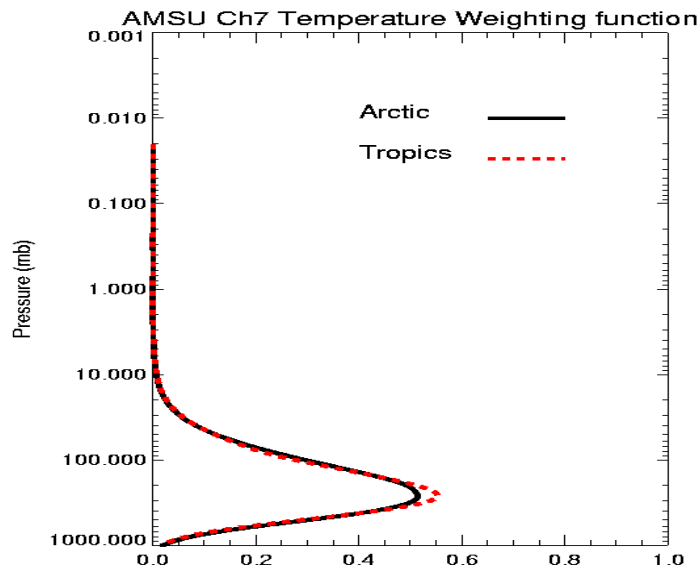


**Figure 2: AMSU Channel 7 Atmospheric weighting functions for a typical atmospheric profile in the Tropics and the Arctic, respectively. The weighting function is defined as  $d(\text{transmittance})/d\ln(p)$ .**

Because the shape and magnitude of MSU/AMSU temperature WF is also a function of viewing geometry, the satellite viewing angle is set to nadir for our calculations. Only AMSU channel 7 pixels with viewing angle within  $\pm 15$  degree are included in the calibration procedure (see section 3.2 step (2)).

To perform the conversion of the high resolution radiosonde temperature profiles into synthetic microwave Tbs, an AMSU fast forward model with 100 fixed pressure levels from CIMSS (microwave forward model-MWF<sub>CIMSS</sub>) (Hal Woolf, CIMSS, personal communication, 2005) was used. Radiosonde soundings are interpolated to MWF<sub>CIMSS</sub> levels with reduced vertical resolution.

Instead of using a fixed AMSU channel 7 or MSU channel 3 weighting function, we apply each radiosonde profile to MWF<sub>CIMSS</sub> to simulate AMSU channel 7 or MSU channel 3 Tbs (TTS). This approach ensures that the potential effects of changing TLS weighting functions at various atmospheric temperature structures to calculated Tbs are minimal.

The MSU/AMSU forward model is applied in two steps. First the temperature and water vapor profiles are extracted from the NCEP ADP Global Upper Air Observational Weather Data and interpolated to the 100 pressure levels of the forward model and stored into daily

data files. Then the forward model is applied to the profiles in each daily file to produce the derived input for the processing algorithm.

In greater detail the steps are:

**STEP(1) Pre-Processing:** The temperature and water vapor data from radiosonde are pre-processed using the IDL program '*extract radiosonde profiles.pro*'. The user must edit this program to specify the time interval of data to process, and the input/output paths for the datasets. The MERRA reanalysis data are firstly pre-processed using the IDL program '*merra\_hdf2sav.pro*' and '*merra\_sav2txt.pro*.' The programs is then compiled and run separately in IDL for each mission and MERRA. The extracted profiles for each mission are interpolated to the 100 pressure levels of the AMSU or MSU forward model. After missing values are replaced using seasonal standard atmosphere profiles, the results are stored into daily ASCII files for later use.

**STEP(2) Apply AMSU/MSU Forward Model:** Temperature and water vapor profiles from radiosonde or MERRA are then passed to the AMSU/MSU forward model to calculate brightness temperatures for AMSU or MSU channels. The FORTRAN program reads in the profile data for the given time interval. The resulting brightness temperatures for each day are written to ASCII files for later use as input to the processing algorithm.

### 3.3.4 Forward Models

In this study, temperature and water vapor profiles from NCEP ADP Global Upper Air Observational Weather Data (from 2001 June to December 2012) are used to compute the synthetic AMSU Ch7 Tbs. All radiosonde profiles were downloaded from the CISL Research Data Archive. The MERRA reanalysis data from 1980 to 2004 are used to generate MSU Ch3 Tbs and data from 2001 to 2014 generate the AMSU Ch7 Tbs. The MSU and AMSU fast forward models from the Cooperative Institute for Meteorological Satellite Studies–CIMSS, MWFCIMSS (Hal Woolf, CIMSS, personal communication, 2005) are used to project each radiosonde profile into synthetic microwave Tbs. The validation of microwave transmittance of this model is described in Woolf et al. (1999).



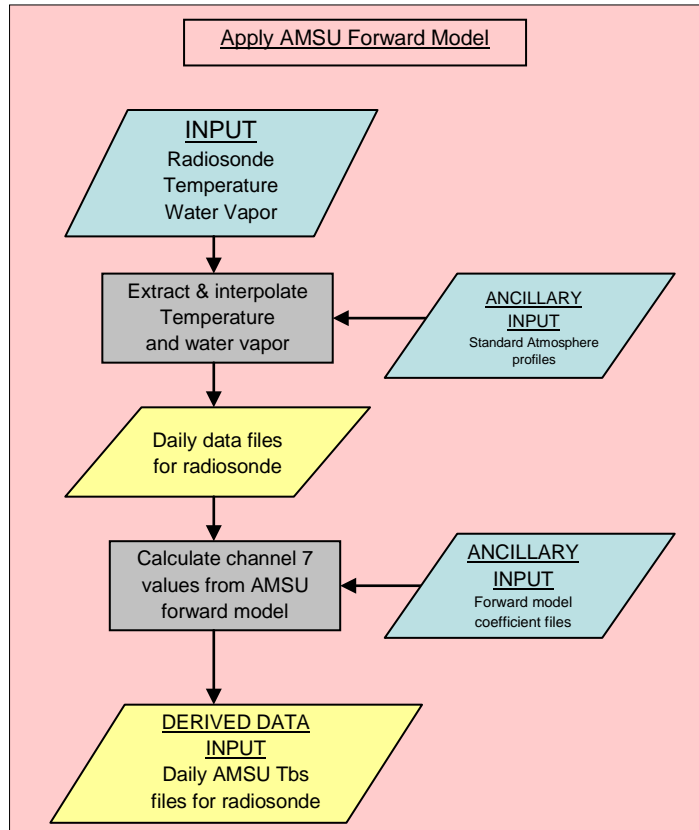


**Figure 3: Flow chart of the procedures to use radiosonde data to AMSU forward model to compute the simulated AMSU Channel 7 Tbs.**

## 3.4 Theoretical Description

The objective of this algorithm is to use GPS RO data to serve as climate benchmark to identify high quality RAOBs and use the RO identified RAOBs to calibrate AMSU/MSU TTS measurements. The high quality RAOB temperature profiles are used to vicariously calibrate AMSU/MSU measurements to constrain the uncertainties of satellite-inferred stratospheric and tropospheric temperature trends.

### 3.4.1 Physical and Mathematical Description

Raw RO observations and precise positions and velocities of GPS and LEO satellites, can be used to derive atmospheric refractivity profiles, which are a function of atmospheric temperature and moisture profile (Hajj et al., 2004; Kuo et al., 2004; Ho et al., 2009a). In a neutral atmosphere, the refractivity (N) is related to the pressure (P), the temperature (T)

and the partial pressure of water vapor ( $P_w$ ) by the following equation (Bean and Dutton, 1966):

$$N = 77.6 \frac{P}{T} + 3.73 \times 10^5 \frac{P_w}{T^2} \quad (1)$$

The so-called “dry temperature” is obtained by neglecting the water vapor term in equation (1). Above the upper troposphere where moisture is negligible, the dry temperature and the actual temperatures are nearly equal (Ware et al., 1996). Because the fundamental observable for the GPS RO technique is of high precision and stability that can be traced to the SI unit of second, RO data do not contain mission-dependent biases. This is demonstrated by the collocated soundings of the CHAMP (launched in 2001) and the COSMIC (launched in 2006) agreeing to within 0.1 K after retrieval (Anthes et al., 2008; Foelsche et al., 2009; Ho et al., 2009a). This makes them potentially useful as a climate benchmark (Ho et al., 2007, 2009c) in addition to being well suited for detecting climate trends (Ho et al., 2009b).

Here we compare temperature profiles derived from GPS RO data from the COSMIC from 2006 to 2012 and CHALLENGING Minisatellite Payload (CHAMP) from 2001 to 2008 with those from different types of radiosonde systems from 12 to 25 km to assess the performance of these radiosonde systems in the upper troposphere and lower stratosphere. Because GPS RO data are not affected by the temperature variation of the satellite component, we are also able to identify the radiosonde temperature biases due to possible radiative errors resulting from instrument characteristics for different types of radiosonde systems. Because of different solar absorptivity and infrared emissivity, different radiosonde sensor systems actually contain different radiative biases. Figure 4 shows that Vaisala-RS92 does not contain obvious radiative biases (obvious day/night biases) comparing to the collocated RO temperature results in the same height.

An inter-calibration approach using simultaneous nadir overpass (SNO) matchups (Zou et al., 2009; Zou and Wang, 2011) are used to reduce intersatellite biases and warm target temperature contamination of MSU.

The calibration algorithm (see Eq. (2)) are used for converting the raw observations (digital counts) to the radiances:

$$(2)$$

where  $R$  is the final earth scene radiance;  $R_L = R_c + S(C_e - C_c)$  representing the dominant

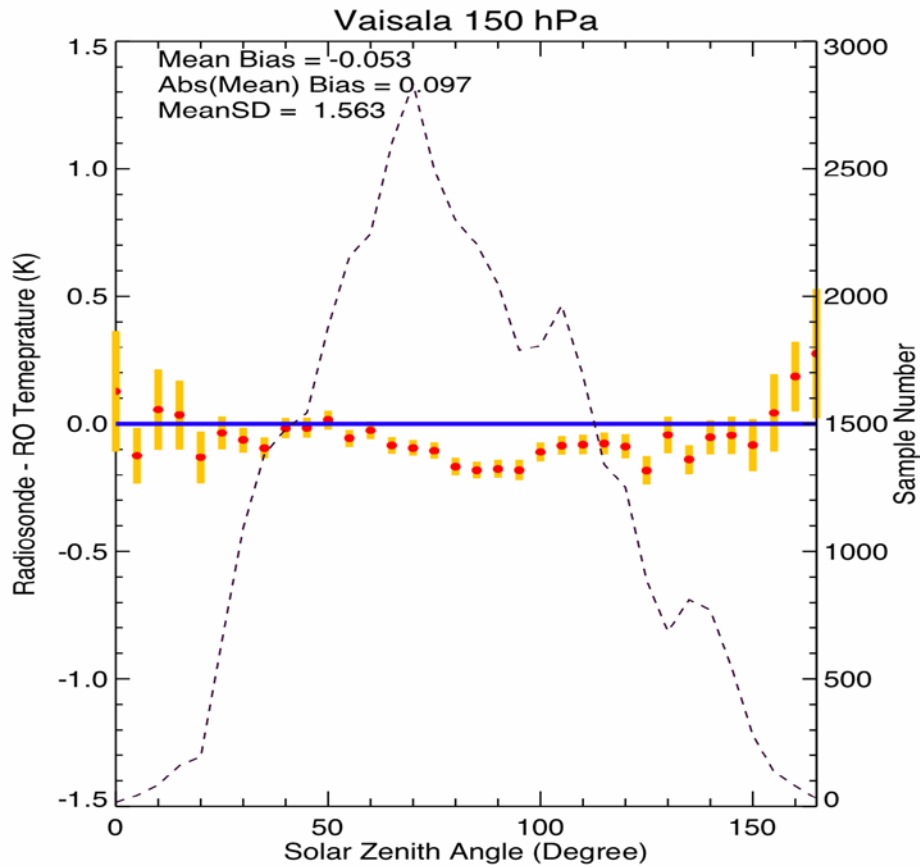


**Figure 4: Temperature comparisons between COSMIC and radiosonde at 150 hPa for Vaisala-RS92 from 2002 to 2008. The red dot is for the mean difference, the orange line is for the standard deviation, and the dotted line is the sample number for RO and radiosonde pairs in that height.**

linear response and  $S = (R_w - R_c) / (C_w - C_c)$  is the slope;  $Z = S^2(C_e - C_c)(C_e - C_w)$  is a nonlinear response;  $C$  represents the raw counts data of the satellite observations; The subscripts  $e$ ,  $w$  and  $c$  refer to the earth-view, onboard warm blackbody target view, and cold space view, respectively.  $\delta R$  represents a radiance offset.  $\mu$  is the nonlinear coefficient.

The radiance offset  $\delta R$  and nonlinear coefficient  $\mu$  are assumed to be constant. And the bias of radiance between satellites can be written as:

$$\Delta R_{m,n} = \Delta R_{Lm,n} + (\delta R_m - \mu_m Z) - (\delta R_n - \mu_n Z) \quad (3)$$

The SNO matchups between NOAA missions are used to generate the  $\Delta R_{m,n}$  and  $\Delta R_{Lm,n}$  for all match pairs. The  $\delta R$  for NOAA14 are assumed as 0. So for a given  $\mu$  for NOAA14 the  $\delta R$  and  $\mu$  for NOAA 12 can be generated by solve the equation (3). Then  $\delta R$  and  $\mu$  of NOAA 11 can be obtained with SNO matchups of NOAA12 and NOAA11. The procedure is continued until  $\delta R$  and  $\mu$  for all MSU missions are generated. The SNO matchups contain simultaneous observations over the polar region that are less than 2 minutes apart and within 111 km from any NOAA satellite pairs.

The MERRA simulated gridded Tbs are interpolated to the time, location and satellite zenith angle for each MSU measurement ( $T_{MSU}(t, lon, lat, lza)$ ,  $T_{AMSU}(t_0, lon, lat, lza_0)$ ). The  $t$ ,  $lon$ ,  $lat$ ,  $lza$  represent the local time, longitude, latitude, satellite zenith angle for the measurement. The MSU channel 3 Tbs are corrected to the local time  $t_0$  and satellite zenith angle  $lza_0$  which are set to 0 and converted to AMSU channel 7 Tbs:

$$T_c = T + T_{AMSU}(t_0, lon, lat, lza_0) - T_{MSU}(t, lon, lat, lza) \quad (4)$$

The SNO method can not remove all the biases of Tbs for MSU missions. So a modified Christy method is used which is updated from the method used by Christy et al. (2000). Radiosonde simulated data are used as 'real' to calibrate the Tbs in this method. To reduce the seasonal dependent biases of MSU Tbs the seasonal bias  $B_{season}$  are introduced in the calibration algorithm. A coefficient of trend ( $t_m$ ) of bias is concerned in the calibration. The biases for matched Radiosonde simulated Tbs and NOAA Tbs ( $T_m$ ) can be written as:

$$\Delta T_{raob,m} = bias_{raob,m} - a_m T_{Wm} - s_m B_{season} - t_m Time \quad (5)$$

And biases of Tbs between and NOAA satellites can be written as:

$$\Delta T_{m,n} = bias_{m,n} + a_m T_{Wm} + s_m B_{season} + t_m Time - a_n T_{Wn} - s_n B_{season} - t_n Time \quad (6)$$

Where  $T_w$  is the warm target temperature. In the equation (5), the subscript  $m$  represents NOAA14 for MSU. In the equation (6), the subscripts  $m$  and  $n$  represent from NOAA14 to TIROS.  $B_{season}$ , which is a function of month, is generated by differences of Tbs between radiosonde simulated and NOAA14.  $a$  and  $s$  represent coefficients for warm target and seasonal biases.  $bias_{raob,m}$  and  $bias_{m,n}$  represent the offset for Tbs between NOAA satellites.  $Time$  is the number of days from January 1, 1980. The equations are solved simultaneously to generate the  $bias_{raob,m}$ ,  $bias_{m,n}$ , and linear coefficients  $a$ ,  $s$ ,  $t$  for each mission. Then the calibrated Tbs can be written as:

$$\begin{aligned} T_{14c} &= T_{14} - a_{14} T_{W14} - s_{14} B_{season} - t_{14} Time + bias_{raob,14} \\ T_{12c} &= T_{12} - a_{12} T_{W12} - s_{12} B_{season} - t_{12} Time + bias_{14,12} + bias_{raob,14} \\ T_{11c} &= T_{11} - a_{11} T_{W11} - s_{11} B_{season} - t_{11} Time + bias_{12,11} + bias_{14,12} + bias_{raob,14} \end{aligned} \quad (7)$$

and so on ...

Then  $\mu$  for reference mission are selected corresponding the smallest standard deviation of inter-satellite biases for all the missions.

### **3.4.2 Data Merging Strategy**

Monthly gridded values for each polar orbiter are calculated by binning and averaging pixel level data. The combined monthly average for all polar orbiters is calculated by a simple average of the gridded values from each orbiter.

### **3.4.3 Numerical Strategy**

N/A

### **3.4.4 Calculations**

The calculations primarily consist of binning, averaging, regression, and linear fitting of data points.

### **3.4.5 Look-Up Table Description**

N/A

### **3.4.6 Parameterization**

N/A

### **3.4.7 Algorithm Output**

The algorithm results consist of a set of netCDF files, one for each month over the time interval from Jan 1980 through December 2013. Each file contains the combined calibrated AMSU channel 7 mean brightness temperatures (K) from available polar orbiters on a 2.5x2.5 degree grid. Also contained in the files are the number of AMSU observations for each gridpoint, the latitudes and longitudes of gridpoints, and the month, year. Each of the 116 files uses less than 100Kb.

## 4. Test Datasets and Outputs

### 4.1 Test Input Datasets

Two months of test data from November and December of 2006 are provided with the IDL and FORTRAN source programs. The directory *\$SRC/Test-Data/Input/AMSU/* contains sub-directories containing L1B polar orbiter data for NOAA-15, NOAA-16, NOAA-18, and AQUA. The directory *\$SRC/Test-Data/ASCII tmp/gps AMSU Tbs/* contains the derived AMSU brightness temperatures from the COSMIC and CHAMP GPSRO missions. These are the input data used by the processing algorithm. The other directories; *extract/*, *match/*, *offset\_slope/*, and *bin/* in the *\$SRC/ASCII tmp/* directory contain the intermediate processing results from each IDL program for these two months. The final netCDF results are contained in the *\$SRC/Test-Data/Output/* directory.

### 4.2 Test Output Analysis

#### 4.2.1 Reproducibility

Along with the two months of level 1B AMSU data and GPS RO derived brightness temperatures, all of the intermediate datasets generated during processing leading up to the final results are provided. Applying the processing algorithm to the input datasets, the user should recover exact results for each of these intermediate files. Differences in any of these intermediate or final results are indicative of an error.

#### 4.2.2 Precision and Accuracy

##### 4.2.2.1 Precision and Accuracy of RO Data

Kuo et al. (2004) showed that GPS RO soundings have very high accuracy (up to 0.3% in terms of refractivity) in the layer between 5 to 25 km. Ho et al., (2009a) showed that collocated CHAMP and COSMIC dry temperature differences between 500 hPa and 10 hPa range from -0.35 K (at 10 hPa) to 0.25 K (at 30 hPa) and their mean difference is about -0.034 K. The fact that the mean dry temperature difference in the height ranging from 500 hPa to 10 hPa is within the normalized standard error of the mean difference demonstrates long-term stability of the GPS RO signals. In addition, to quantify the accuracy of RO temperature profile, we compared RO temperature profiles collocated with high quality radiosonde data. Temperature comparison between COSMIC and temperature measurements from Vaisala-RS92 show that COSMIC temperature is very close to those of

radiosondes from 200 hPa to 20 hPa (around 12 km to 25 km) with a zero mean (He et al., 2009; Ho et al., 2010, also see Figure 4).

#### **4.2.2.2 Precision of RAOB simulated TTS to the observed AMSU TTS**

The feasibility of this approach depends on the quality of the RAOB simulated TTS and the fitness (i.e., high correlation coefficient, and the small standard deviation) between the RAOB simulated TTS to the observed AMSU TTS.

Five types of Vaisala radiosonde data from the year of 2001 to 2012 were used to calibrate TTS taken from AMSU measurements from different satellites for potential improvements of troposphere and stratosphere temperature trend analysis. Figure 5 depicts the comparison of synthetic RAOB Tbs with AMSU N15, N16, and N18 Ch7 Tbs. The slope and offset from each of the RAOB and AMSU TTS pairs are used to convert the observed AMSU TTS to calibrated AMSU TTS for each of the missions. To avoid anomalous values due to missing data, differences in brightness temperatures larger than 10 degrees are omitted. Collectively these parameters balance the tradeoff between the quality and the number of the matched measurements.

To avoid the spatial and temporal representation errors, we collocate AMSU pixels with each RAOB profile within 30 minutes and 50 km. AMSU pixels with a satellite viewing angle ranging from -15 degrees to 15 degrees are all included in this study to increase the number of AMSU pixels in our comparison. The comparison results show that the RAOB simulated TTS is highly correlated with those of the AMSU observed TTS. For example, the correlation coefficient for the RAOB and N15 TTS pairs is equal to 0.99 with a mean bias of 0.72 K and a standard deviation of 0.4 K. The RAOB-N16 pairs and the RAOB-N18 pairs are of the similar correlation coefficients ( $\sim 0.996$ ) and standard deviations (less than 0.5 K). The mean biases for RAOB-N15, RAOB-N16, and RAOB-N18 pairs are 0.72K, 1.01 K, and 1.3 K, respectively. This is reflecting the inter-satellite biases among N15, N16, and N18 TTS.

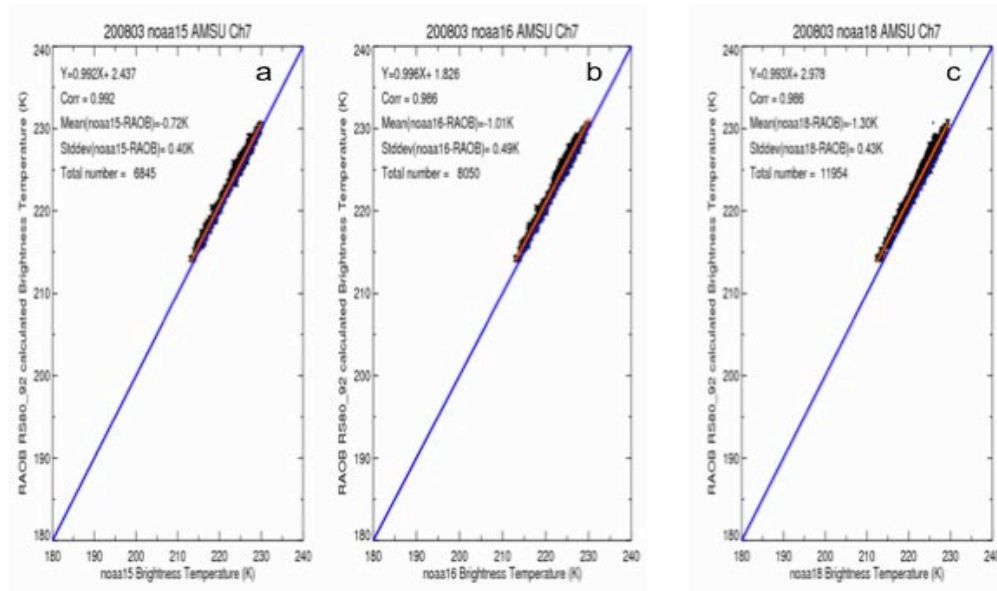


**Figure 5: Comparison of synthetic RAOB Tbs and (a) AMSU N15 Ch7 Tbs, (b) AMSU N16 Ch7 Tbs, (c) AMSU N18 Ch7 Tbs.**

### 4.2.3 Error Budget

N/A



## **5. Practical Considerations**

### **5.1 Numerical Computation Considerations**

IDL is not well suited to take full advantage of SMP environments. Since the computationally intense programs typically have to be run separately for each RO mission or polar orbiter, processing is optimized by simultaneously running separate IDL sessions.

### **5.2 Programming and Procedural Considerations**

Execution of the IDL programs requires that the user edit the program file to specify the run parameters controlling execution. Programs must then be compiled and run from within an IDL session.

### **5.3 Quality Assessment and Diagnostics**

In addition to the fitness (i.e., high correlation coefficient, and the small standard deviation) between the RAOB simulated TTS to the observed AMSU TTS, the feasibility of this approach also depends on the long-term stability of the RAOB data. To assess the quality especially long-term stability of the RAOB data, we compare the RO temperature profiles to those high quality RAOB temperature profiles from 8 km to 25 km from 2001 to 2010. We assume the long-term stability of RAOB data below 8 km is consistent with those above 8 km altitude.

In the performance period, we continue refining the AMSU ch7/MSU ch3 calibration algorithm. Because RO temperature is less affected by moisture amount above 8 km, we first use RO temperature profiles to collocate with different radiosonde (RAOB) types and identify high quality of RAOB data and use those data to calibrate AMSU ch7 Tbs from different satellite missions. Figure 6 shows time series of monthly mean temperature bias between radiosonde of Vaisala RS92 and GPS RO data at 50 hPa from 2006 to 2010. In general, temperature measurements from RS92 are very consistent with those of collocated RO temperature from 2006 to 2012 (not shown). Except in the Tropics, the mean biases between RS92 and RO temperatures are within  $\pm 0.25\text{K}$ . We have repeated the similar comparisons to all those five radiosonde types whenever they are collocated with RO data.

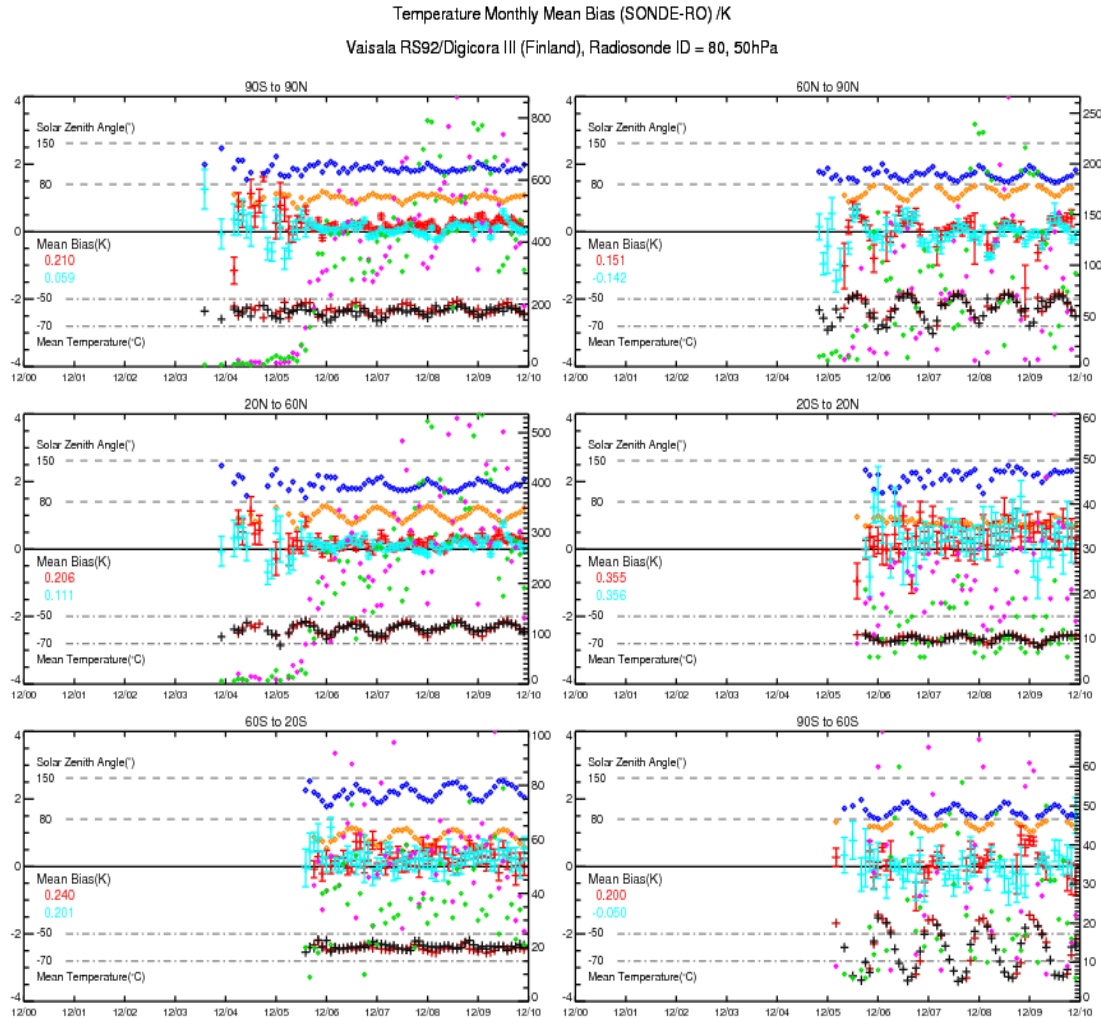


**Figure 6: The differences of temperature between RS92 and collocated GPS RO at 50 hPa for the global (upper left panel), 90°N to 60°N zone (upper right panel), 20°N to 60°N zone (middle left panel), 20°N to 20°S zone (middle right panel), 60°S to 20°S zone (lower left panel), and 90°S to 60°S zone (lower right panel). The red dots are for the day time RS92-RO temperature biases and the blues dots are for the night time RS92-RO temperature biases.**

## 5.4 Exception Handling

The program will stop and print out an informative message for all *known* error conditions.

## 5.5 Algorithm Validation

Using identified RAOB types from 2001 to 2014, we compute the forward calculated AMSU ch7 Tbs. The RAOB simulated AMSU ch7 Tbs and AMSU Tbs are matched to generate the linear fit coefficients which are used to calibrate AMSU ch7 Tbs from NOAA15, 16, 18, 19, Metop-A.

For MSU data from TIROS, NOAA6, NOAA7, NOAA8, NOAA9, NOAA10, NOAA11, NOAA12, and NOAA14, the SNO method is used to calibrate all MSU missions to NOAA14. Then the MERRA simulated MSU ch3 Tbs and AMSU ch7 Tbs are used to the limb correction, locate time correction and conversion of MSU ch3 to AMSU ch7. GPS-RO identified RAOB simulated AMSU ch7 Tbs from 2001 to 2004 are used as the benchmark to calibrate the remaining inter-satellite biases and seasonal variations of biases with a modified Christy method.

After using RAOB calculated ch7 Tbs to calibrate those for AMSU ch7 Tbs for each satellite missions, the inter-satellite biases among missions are within  $\pm 0.5\text{K}$  globally.

Figure 7 shows the time series of MSU/AMSU TTS Tbs between N6-TIROS, N7-N6, N8-N7, N9-N8, N10-N9, N11-N10, N12-N11, N14-N12, N16-N15, N18-N15, N19-N15, Metop-A – N15 for the global (upper left panel), 90° N to 60° N zone (upper right panel), 20° N to 60° N zone (middle left panel), 20° N to 20° S zone (middle right panel), 60° S to 20° S zone (lower left panel), and 90° S to 60° S zone (lower right panel) from 1980 to 2013.

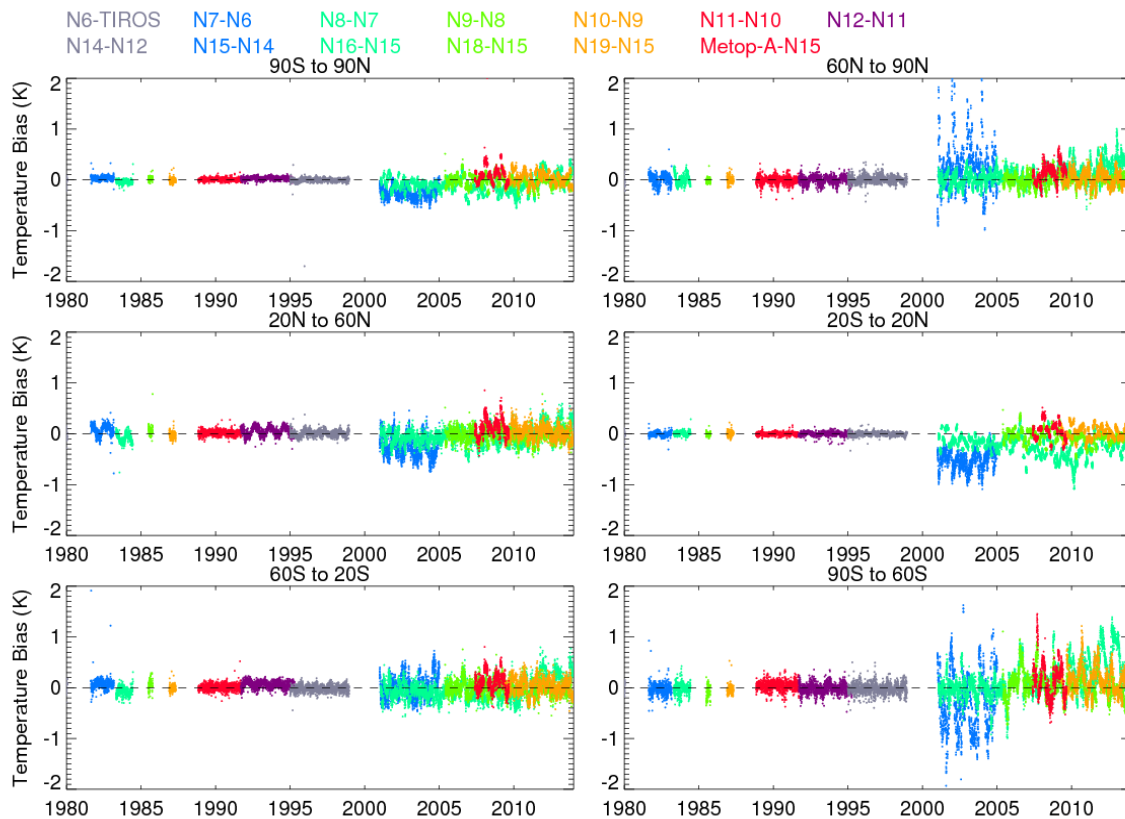


**Figure 7: The time series of MSU/AMSU TTS Tbs between N6-TIROS, N7-N6, N8-N7, N9-N8, N10-N9, N11-N10, N12-N11, N14-N12, N16-N15, N18-N15, N19-N15, Metop-A - N15 for the global (upper left panel), 90° N to 60° N zone (upper right panel), 2° N to 60° N zone (middle left panel), 20° N to 20° S zone (middle right panel), 60°S to 20° S zone (lower left panel), and 90° S to 60° S zone (lower right panel).**

## 5.6 Processing Environment and Resources

IDL version 7.1 was used to process the data on a x86\_64 server running the CentOS operating system. The ASCII temporary data files require about 7Gb of disk space per month.

## **6. Assumptions and Limitations**

The algorithm assumes that there are a sufficient number of coincident measurements during each month to provide a statistically reliable estimate of slope and offset values.

### **6.1 Algorithm Performance**

N/A

### **6.2 Sensor Performance**

N/A

## **7. Future Enhancements**

### **7.1 Enhancement 1- Improve Algorithm Usage**

To avoid processing errors which result from the user having to edit and re-run programs for different GPSRO missions, polar orbiters, time intervals, etc., The algorithm should be restructured to utilize a single configuration file containing RUN parameters used by all of the processing programs. A single processing program should then implement the algorithm by calling each of the current processing programs as subroutines. Intermediate data file should be stored in a more robust format, which does not use so much disk space.

### **7.2 Enhancement 2– Further Validation**

To assess the quality of the derived TTS record, we will compare the derived TTS results with other TTS datasets. We will compare our derived TTS results with those newly available TTS datasets provided by RSS (Remote Sensing System Inc.) and TTS processed by NOAA Center for Satellite Applications and Research (STAR, using simultaneous nadir overpass-SNO method) from 1980 to 2014. This is to demonstrate the quality of the derived TTS record.

## 8. References

- Anthes, R. A., and Coauthors (2008), The COSMIC/FORMOSAT-3 Mission: Early Results. *Bul. Amer. Meteor. Soc.*, 89(3), 313-333.
- Bean, B.R., E. J., Dutton (1966), Radio Meteorology; National Bureau of Standards Monogr. 92; US Government Printing Office: Washington, DC, USA, 1966.
- Christy J.R., Spencer R.W., Braswell W.D. (2000) MSU Tropospheric Temperatures: Dataset Construction and Radiosonde Comparisons. *Journal of Atmospheric and Oceanic Technology* 17:1153-1170. DOI: 10.1175/1520-0426.
- Christy, J. R., R. W. Spencer, W. B. Norris, W. D. Braswell, and D. E. Parker (2003), Error estimates of Version 5.0 of MSU/AMSU bulk atmospheric temperatures. *J. Atmos. Oceanic Technol.*, 20, 613–629.
- Foelsche, U., B. Pirscher, M. Borsche, G. Kirchengast, and J. Wickert (2009), Assessing the Climate Monitoring Utility of Radio Occultation Data: From CHAMP to FORMOSAT-3/COSMIC. *Terr. Atmos. Oceanic Sci.*, 20, 155-170.
- Hajj, G. A., and Coauthors (2004), CHAMP and SAC-C atmospheric occultation results and intercomparisons. *J. Geophys. Res.*, 109, D06109, doi:10.1029/2003JD003909.
- He, W., S. Ho, H. Chen, X. Zhou, D. Hunt, and Y. Kuo (2009), Assessment of radiosonde temperature measurements in the upper troposphere and lower stratosphere using COSMIC radio occultation data, *Geophys. Res. Lett.*, 36, L17807, doi:10.1029/2009GL038712.
- Ho, S.-P., Y. H. Kuo, Zhen Zeng and Thomas Peterson (2007), A Comparison of Lower Stratosphere Temperature from Microwave Measurements with CHAMP GPS RO Data, *Geophys. Research Letters*, 34, L15701, doi:10.1029/2007GL030202.
- Ho, S.-P., M. Goldberg, Y.-H. Kuo, C.-Z Zou, W. Schreiner (2009a), Calibration of Temperature in the Lower Stratosphere from Microwave Measurements using COSMIC Radio Occultation Data: Preliminary Results, *Terr. Atmos. Oceanic Sci.*, Vol. 20, doi: 10.3319/TAO.2007.12.06.01(F3C).
- Ho, S.-P., G. Kirchengast, S. Leroy, J. Wickert, A. J. Mannucci, A. K. Steiner, D. Hunt, W. Schreiner, S. Sokolovskiy, C. O. Ao, M. Borsche, A. von Engeln, U. Foelsche, S. Heise, B. Iijima, Y.-H. Kuo, R. Kursinski, B. Pirscher, M. Ringer, C. Rocken, and T. Schmidt (2009b), Estimating the Uncertainty of using GPS Radio Occultation Data for Climate Monitoring: Inter-comparison of CHAMP Refractivity Climate Records 2002-2006 from Different Data Centers, *J. Geophys. Res.*, doi:10.1029/2009JD011969.
- Ho, S.-P., W. He, and Y.-H. Kuo (2009c), Construction of consistent temperature records in the lower stratosphere using Global Positioning System radio occultation data and microwave sounding measurements, in *New Horizons in Occultation Research*, edited by A. K. Steiner et al., pp. 207–217, Springer, Berlin, doi:10.1007/978-3-642-00321-9\_17.

- Ho, S.-P., Y. H. Kuo, W. Schreiner, X. Zhou (2010) Using SI-traceable Global Positioning System Radio Occultation Measurements for Climate Monitoring [In “States of the Climate in 2009”]. *Bul. Amer. Meteor. Sci.*, in press.
- Kuo, Y. H., T. K. Wee, S. Sokolovskiy, C. Rocken, W. Schreiner, D. Hunt, 2004: Inversion and Error Estimation of GPS Radio Occultation Data. *J. of the Meteor. Society of Japan*, 82(1B), 507-531.
- Kursinski, E.R., G.A. Hajj, J.T. Schofield, R.P. Linfield, and K.R. Hardy (1997), Observing Earth’s atmosphere with radio occultation measurements using the Global Positioning System, *J. Geophys. Res.*, 102, 23,429–23,465.
- Ohring, G., Ed., (2007), *Achieving Satellite Instrument Calibration for Climate Change*. National Oceanographic and Atmospheric Administration, 144 pp.
- Woolf, H., P. van Delst, W. Zhang (1999), NOAA-15 HIRS/3 and AMSU Transmittance Model Validation. Technical Proceedings of the International ATOVS Study Conference, 10th, Boulder, CO, 27 January-2 February 1999. Bureau of Meteorology Research Centre, Melbourne, Australia, 1999, pp.564-573.
- Zou C.-Z., Gao M., Goldberg M.D. (2009) Error Structure and Atmospheric Temperature Trends in Observations from the Microwave Sounding Unit. *Journal of Climate* 22:1661-1681. DOI: 10.1175/2008jcli2233.1.
- Zou C.Z., Wang W.H. (2011) Intersatellite calibration of AMSU-A observations for weather and climate applications. *Journal of Geophysical Research-Atmospheres* 116. DOI: Artn D23113, Doi 10.1029/2011jd016205.



## Appendix A. Acronyms and Abbreviations

<b>Acronym or Abbreviation</b>	<b>Meaning</b>
AMSU	Advanced Microwave Sounder Unit
Aqua	Aqua (EOS PM-1) is a multi-national NASA scientific research satellite in orbit around the Earth
C-ATBD	Climate Algorithm Theoretical Basis Document
CDR	Climate Data Record
CHAMP	Challenging Mini-satellite Payload
CIMSS	Cooperative Institute for Meteorological Satellite Studies
COSMIC	Constellation Observing System for Meteorology, Ionosphere, and Climate
GCOS	Global Climate Observing System
GPS	Global Positioning System
IDL	Interface description language. This is a specification language used to describe a software component's interface
LECT	Local equator crossing times
LEO	low-Earth orbiting
MERRA	Modern-ERA Retrospective analysis for Research and Applications
MetOP-A	METeorological Operational satellite-A
MSU	Microwave Sounding Unit
MWF	Microwave Forward Model
NASA	National Aeronautics and Space Administration
NCDC	National Climatic Data Center
NESDIS	National Environmental Satellite, Data, and Information Service
NOAA	National Oceanic and Atmospheric Administration
NRC	National Science Council
RAOB	Radiosonde Observation
RSS	Remote Sensing System Inc.
SI	System of Units
SNO	Simultaneous Nadir Overpass

SSEC	Space Science Engineer Center
STAR	Center for Satellite Applications and Research
Tb	Brightness Temperatures
TLS	Temperatures in the Lower Stratosphere
TTS	Temperatures of Troposphere / Stratosphere
UAH	University of Alabama in Huntsville